PAPER ID: 0403
DOI: 10.18462/iir.compr.2021.0403

Process Simulation and Analysis of a Rotary -Vane Gas Refrigerating Machine for Cold Production in the Medium Temperatures Level

Mykhailo Khmelniuk [(a)], Volodymyr Trandafilov [(a)]

[(a)] Odessa National Academy of Food Technologies
Odessa, st. Kanatnaya, 112, 65039, Ukraine, e-mail [vlad.trandafilov@gmail.com]

ABSTRACT

The paper is devoted to the Stirling Refrigeration machines (SRM) for cold production in the medium temperature range (173 to 273 K). To achieve this goal structural optimization of the SRM system is performed and a fundamentally new rotary-vane design of a gas refrigerating machine is proposed. The process model simulation (PMS) of rotary-vane gas refrigerating machine (RVGRM) is developed and presented. The measurement's uncertainty from the theoretical and computer PMS is not more than 5%, which indicates not only the qualitative data convergence, but also the quantitative. At the fixed cooling capacity (12 kW), the RVGRM efficiency is by 15 % higher than piston SRM. Estimated mass and dimension paramaters are by 2.5 times improved. The RVGRM processes analysis for the helium, nitrogen, and methane was carried out. Replacing helium with nitrogen, both cooling capacity and Carnot efficiency (ε) are decreased by 30% and by 6% respectively.

Keywords: Stirling refrigerating machine, rotary - vane gas refrigerating machine, mass-dimensional characteristics, mathematical model, life cycle.

INTRODUCTION

At present, there is a need for refrigerators with a relatively low cooling capacity (about 10 kW) at a temperature level of 0...-100°C (273...173 K). Such type of refrigerators can be designed on the cascade Vapor-Compressor Refrigerating Machines (VCRM) basis with environmently friendly working fluids use. Gas refrigeration machine which the Stirling cycle implements can be an alternative to VCRM.

The multilevel aproach shows that the cascade VCRM due to their complexity and multiple cunstructural element will not be sufficiently relable. In the specified temperature range Stirling Refrigeration Machines (SRM) are characterized by low efficiency, as they are created to achieve lower temperatures, starting from 90K to 4K [1-7]. In addition, Stirling refrigeration machine are based on the reciprocating motion of the pistons realized by a crank mechanism. The complexity of the system cranks and levers limits their widespread use in piston SRM, among other reasons [8, 9].

The purpose of this study is to create and improve a more efficient refrigerator - a rotary vane gas refrigeration machine (RVGRM). Principle of its work, mathematical models of the main processes, energy characteristics and design were considered.

1. RVGRM ELEMENTS AND OPERATION

As prototype for mathematical model development and developing the design of a RVGRM, the SRM with a harmonic drive was taken [10, 11]. In an ideal cycle there are no technical losses [12], a thermodynamic cycle is realized, consisting of two isotherms and two isochores (see Fig. 1). On the ambient temperature isotherm T_C and cooling isotherm T_E the compression and expansion processes of the utility are performed. Isochoric processes are carried out in the regenerator.

The RVGRM (see Fig. 2) consists of two working blocks (WB) 1 and 2, in which the working fluid is compressed and expanded with a 45° shift. The working blocks have one common drive shaft 3. The cooler (C) 6 and the refrigerator (R) 7 are connected to the working blocks by lines of compressed high-temperature and expanded cold working fluid. The heat rejected from it by the coolant through line 16 connected to the multiflow heat exchanger (three streams) 6; A heat supply line 17 from the heat sink is connected to the multiflow heat exchanger.

Two diametrically opposite vanes are installed inside each WB (fig. 2). The vanes 4 and 5 in 1st WB form four work chambers 8, 9, 10, 11; the same vanes in 2d WB form the working cavities 12, 13, 14, 15. The cavities of WB 1 and 2, the lines of the cooler 6 and the refrigerator 7 are sealed and filled under excess pressure with a gaseous working fluid, such as helium.

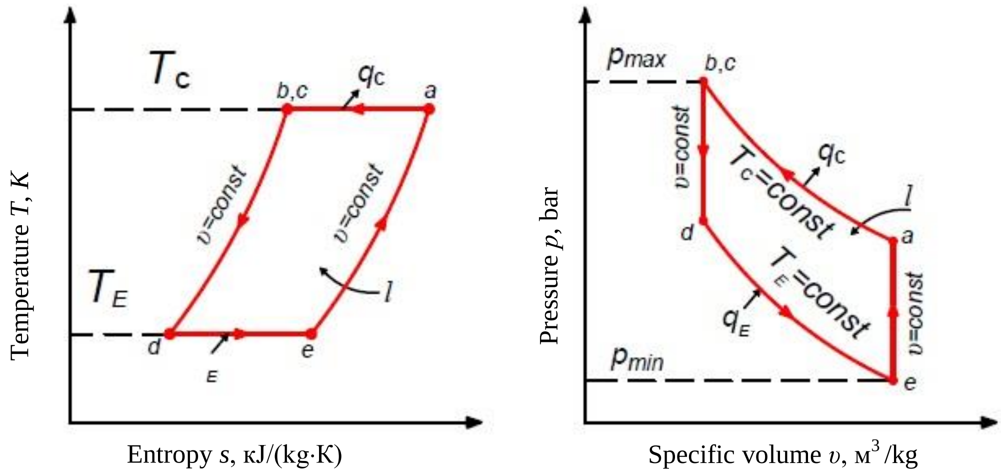

q_C – specific amount of heat removed at T_C, q_E – the specific amount of cold received T_E,
l – specific work expended in the cycle.

Fig. 1. RVGRM thermodynamic cycle in *T–s* and *p–v* coordinates.

During RVGRM operation within the cavities of the first and second working blocks, the processes of compression and expansion are carried out. Fig.1 and Fig.2 show how the working fluid compression and expansion occurs in cavities 15 and 9:

1) gas compression in the cavity 15 WB 2 (process *a* – *b*);
2) the displacement of gas from the cavity 15 through C in WB 1 (point *c*);
3) heat rejected to the environment from the cooler 6;
4) suction gas cooled to T_C from C in the cavity 9 of WB1, where when the gas contacts in 9 of the cold vanes, it is cooled in the process *b* – *d*;
5) expansion of the gas with its simultaneous cooling and implementation of external work (process *d* – *e*);
6) gas injection from the cavity through R in WB 2 (point *e*);
7) heat supply to the gas from the cooled object in R;
8) gas suction from R to the cavity of 15 WB 2, where it is heated in contact with hot vanes in the process *e* – *a*.

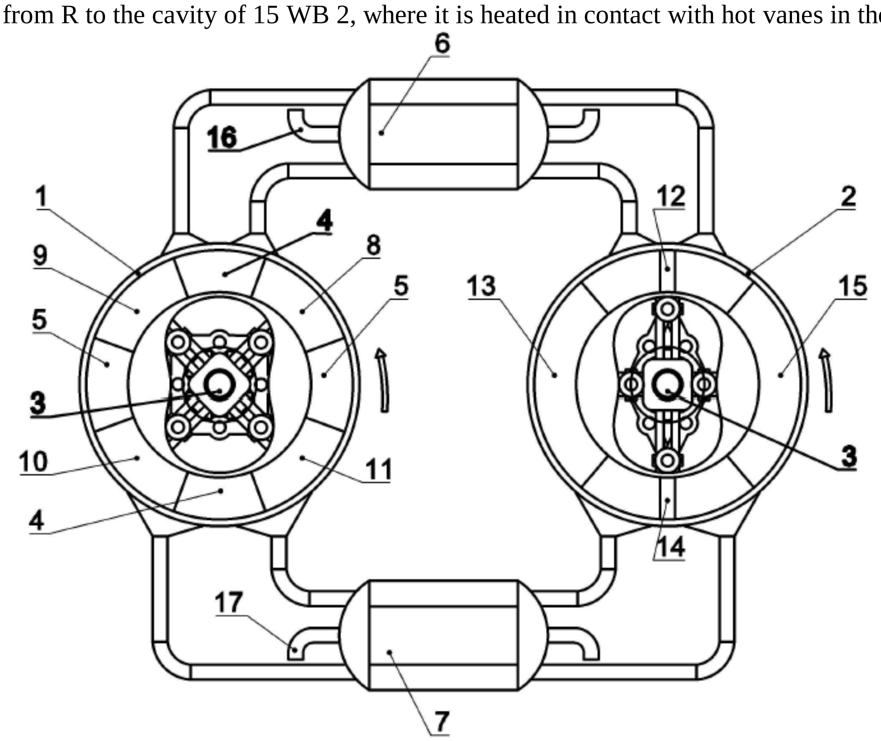

Fig. 2. RVGRM elements.

1, 2 – working blocks, 3 – shaft, 4, 5 – pairs of vanes,
6 – cooler, 7 – refrigerator, 8,9,10,11– cavity WB 1,
12,13,14,15 – cavity WB 2, 16 – heat rejected line, 17 – heat supply line.

Thus, when the rotation of the drive shaft 3 at an angle 90° one complete thermodynamic cycle occurs in WB 1 and 2. With the rotation of the machine drive shaft at 360°, for one revolution, four thermodynamic cycles are performed in the RVGRM.
It follows that the rotary vane gas refrigeration machine implements multidirectional movement of the gaseous working fluid along the path formed by the working cavities of the working blocks 1 and 2 connected through the cooler 6 and the refrigerator 7, thereby eliminating the need for a regenerator (see Fig.1 and Fig.2).
Due to the symmetrical design, the RVGRM is well balanced and creates a minimum level of vibration. Unlike SRM with a connecting rod - piston movement mechanism, there are fewer parts in the RVGRM – corpus and two rotors with vanes. The joining points of moving parts are formed by large surfaces, which makes it easy and reliable to compact them.
In developed RVGRM motion conversion mechanism (MCM)is used which is described in [13]. MCM turns the drive shaft rotation into the rotational-oscillatory motion of the rotors with vanes.
The mechanism consists of a rotating rhomboid and a fixed disk with a profiled raceway (Fig. 3).

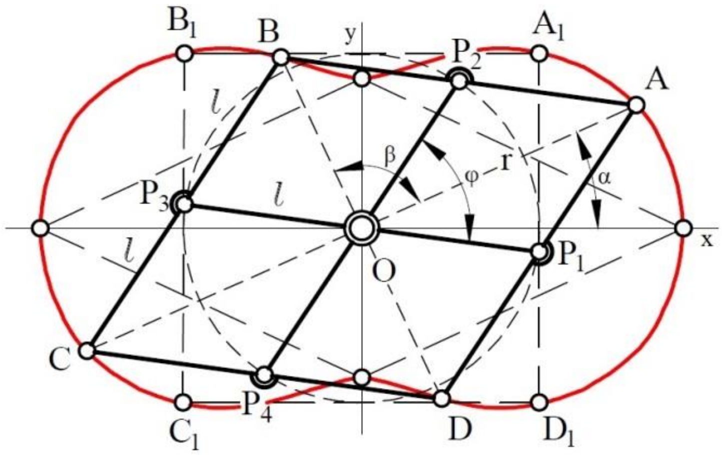

Fig. 3. MCM kinematic scheme.

The rhomboid is comprised of four pivotally connected links of equal length 2*l* (*AB*=*BC*=*CD*=*DA*). By the middle of the links are hinged levers of the vanes, the vanes are called P_1-P_3 and P_2-P_4. Point motion *A, B, C, D* is converted to the movement of points A_1, B_1, C_1, D_1, due to the specific shape of the disk profile.
As the primary angle (rotation angle) the α angle is selected for calculating. The semi-diagonal *r*=*OA* (polar radius) and the angle α between the *OA* and the *x*-axis (polar angle) form the function $r(\alpha)$, thereby setting the theoretical disk profile.
Based on the rhombus properties, the angle β between the diagonals of the rhomboid *OA* and *OB* is constant and equal to $\pi/2$. The change in the angle between the levers $\varphi(\alpha)$ is harmonic with a period equal to π, so the movement of the vanes will be smooth and shockless.

In the developed RVGRM, the profiled disk contour of the MCM with a rhombic drive is described by equation:

$$r = r_A = 2l\cos\left(\frac{\varphi+\beta}{2}\right) \quad (1)$$

Dependence (1) is the basis for the mathematical description of the kinematics of the mechanism for motion conversion of the vanes in the RVGRM working blocks, which affects the nature of the processes implemented in it.
The estimation of the deviation of the theoretical angle φ (α) between the levers and the actual value of the angle between the levers $\overline{\varphi}(\alpha)$ compared to the angle of rotation of the drive shaft α (Fig. 4) was carried out. The maximum differences between them occures at the angle of rotation of the drive shaft $\alpha=\pi/3$ and are about 5°.
Comparison of theoretical and computer data allows to reveal some graphical differences, especially for accelerations of points and links of the mechanism. It results to differences in amplitudes, graphs along the axis, in values at zero angle of drive shaft rotation and for one full revolution. The revealed deviations are explained by the fact that the simulated model is solid-state. When determining velocities and accelerations, it takes into account inertial forces and moments arising during the rotation of the mechanism, as well as the nature of the links interaction of the MCM. The computer model is set by initial conditions that take into account the moments of acceleration and deceleration.

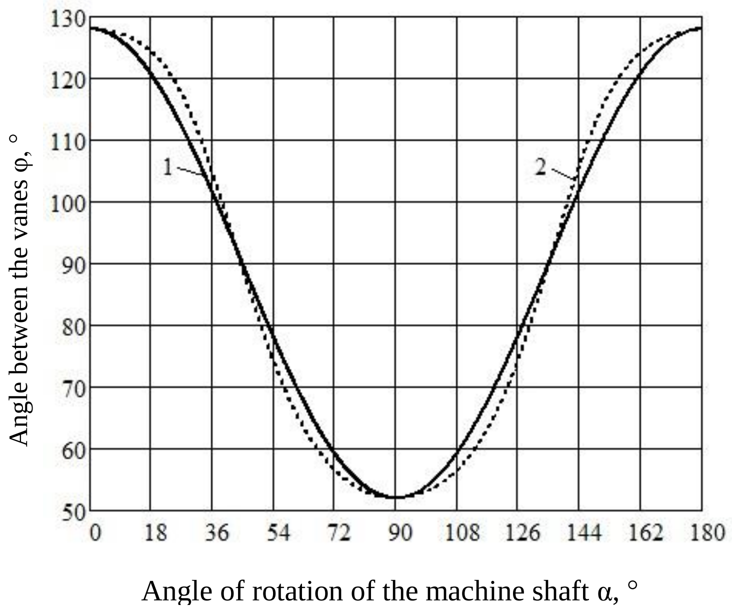

Fig. 4. The dependence of the angle between the arms of the vanes φ on the angle α: 1– theoretical data, 2– computer data.

However, in the results obtained, the differences, as can be seen from Fig. 4, is insignificant (no more than 3%) and can not significantly affect the theoretical indicators. Comparison of graphs confirms their qualitative convergence.

3. MATHEMATICAL MODEL

The SRM developers [14, 15] were the first who set out its thermodynamic features. At first they considered the simplest theoretical machine with the intermittent movement of two working pistons. Using Schmidt's theory (1861) were prepared main characteristics of the idealized machines, working with harmonic drive pistons. The refrigeration coefficient ε of SRM is equal to the refrigeration coefficient of the reversible Carnot cycle ε_c. After that, the values of SRM characteristics were estimated taking into account internal and external irreversibility losses.

Let us first to analyze the RVGRM energy characteristics, which implements an ideal cycle. Then, to determine the RVGRM characteristics as close as possible to those of a real machine, consider its cycle with adiabatic processes of gas compression and expansion.

Using [13], we establish the dependences of the volumes of the cavities on the angle of shaft rotation in the case of rhombic drive use in the conversion motion mechanism for the RVGRM.

Considering the design dimensions of the rotor-vane group for refrigerating machine and the parameters of the conversion movement mechanism, the law of variation of the cavity volume between the vanes is derived from Eq.1 depending on the angle α in the following:

$$V(\alpha) = (2a \cdot \cos 2\alpha + 2b - \varphi_v)\, s \qquad (2)$$

where $a = \pi/4 - \varphi/2$, $b = \pi/4$ – parameters of the profiled contour of the raceway; φ – angle between the arms of the vanes; φ_v – angular size of the vane parameter, s = 0,5· $w_v\,(r_v^2 - r_s^2)$,), w_v – vane width, r_v – vane radius, r_s – shaft radius.

Changes in the volume of cavities in one revolution of the drive shaft (see Fig. 5) are presented for the cavities of the two working blocks of the RVGRM depending on the angle of rotation of the drive shaft.

From Fig. 5 it follows that the shift between the values of $V(\alpha)$ in the first and second WB is 45°.

The volumes at the nodal points of the cycle, in which the beginning and end of each process correspond to the drive shaft rotation on 45°. The result obtained:

$$V_a = V_e = (2a + 2b - \varphi_v)\, s \qquad (3)$$

$$V_b = V_d = (2b - \varphi_v)\, s \qquad (4)$$

where s – refrigeration machine working area parameter.

The processes occurring in the two cavities RVGRM, for example, as shown in Fig. 2, in 15 and 9, are similar to the processes in idealized Stirling refrigeration machine. In [16] the Stirling cycle the pressure p in the working volume of the machine also varies according to the harmonic law:

$$p = p_{\min} \frac{1+\delta}{1+\delta\cos(\alpha-\theta)} \tag{5}$$

where θ – the angle corresponding to the minimum pressure in the cavity, the value of which can be determined from the following:

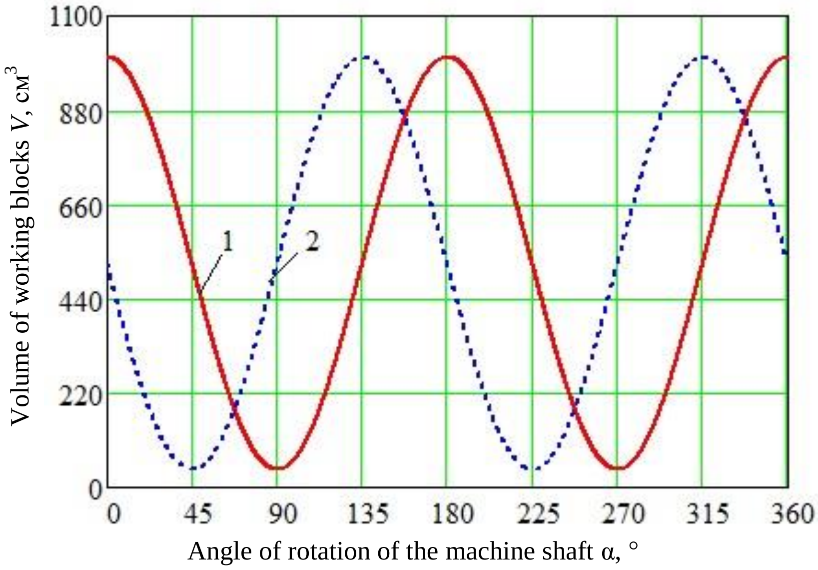

Fig. 5. Changes in the volume of cavities in the WB depending on the angle α: 1, 2 – volumes of the cavities of the first and second WB, respectively.

$$\theta = \mathrm{arctg}\frac{w\cdot\sin\phi}{\tau+w\cdot\cos\phi} \tag{6}$$

δ – design parameter that determines the degree of compression in the cycle:

$$\delta = \frac{\sqrt{\tau^2+2\cdot\tau\cdot w\cdot\cos\phi+w^2}}{\tau+w+2\cdot\bar{a}_\Sigma} \tag{7}$$

w – the ratio of the maximum volumes of compression and expansion cavities, which usually is in the range 1…1,3; ϕ – shift angle changes in volumes of compression and expansion; $\tau = T_C/T_E$ – ratio of temperature of the cooler and the refrigerator; $\bar{a}_\Sigma = \bar{a}_k + \bar{a}_c + \bar{a}_r$ – relative reduced «dead» volume. For further use, we introduce the average pressure in the machine:

$$\bar{p} = p_{\max}\cdot\left[(1-\delta)/(1+\delta)\right]^{1/2} \tag{8}$$

Cooling capacity for RVGRM with a drive having a rotational speed n, min^{-1}:

$$Q_E = \frac{\pi\cdot n}{60}\cdot V_e\cdot\bar{p}\cdot\sin\theta\frac{\delta}{1+\sqrt{1-\delta^2}} \tag{9}$$

where V_e – maximum cavity expansion volume.

The amount of heat rejected from the cooler into the environment,

$$Q_C = \frac{\pi\cdot n}{60}V_e\cdot\bar{p}\cdot w\frac{\delta\sin(\phi-\theta\ )}{1+\sqrt{1-\delta\ ^2}} \tag{10}$$

Having expressions for Q_E and Q_C, found RVGRM idealized coefficient of performance:

$$\varepsilon_S = \left[\left(Q_C / Q_E \right) - 1 \right]^{-1} = \left[\left(T_C / T_E \right) - 1 \right]^{-1} = 1{,}36, \qquad (11)$$

where T_C = 300 K – ambient temperature; T_E = 173 K – cooling temperature.

It follows that the cooling coefficient of an idealized Stirling machine and RVGRM is strictly equal to the refrigeration coefficient of the Carnot cycle. It is caused by the fact that in deriving relations (9) and (10) the losses from irreversibility were not taken into account.

We define, using (9) such characteristic as cooling capacity

$$Q_E = \frac{\pi \cdot 1450}{60} \cdot 1{,}21 \cdot 10^{-3} \cdot 1 \cdot 10^{6} \cdot 0{,}54 \frac{0{,}465}{1 + \sqrt{1 - 0{,}465^2}} = 10{,}9\ kW$$

The derived value Q_E shows that in idealized RVGRM it is possible to reach the cooling capacity about 10 kW at T_E = 173 K (minus 100°C).

In [17, 18], the main losses arising in SRM are combined by the authors into two groups: some of them cause a cooling capacity decrease, and others energy consumption increase. The need to reduce them was indicated in [19].

Fig. 6 represents that losses of this type can occur in a SRM cycle under adiabatic compression of gas from temperature T_C to T_C' 'and adiabatic expansion from T_E to T_E'. It causes a transition from the cycle *1–2–3–4* with isothermal compression and expansion to the cycle *1–2'–2–3–4'–4–1* with adiabatic processes.

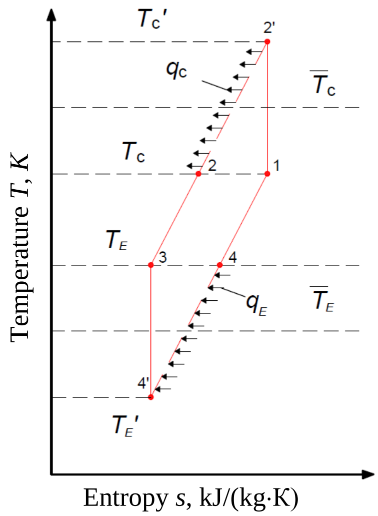

Fig. 6. RVGRM cycle with isothermal and adiabatic gas compression and expansion processes: 1–2–3–4 – reversible cycle of RVGRM with isothermal processes, 1–2'–2–3–4'–4–1 – cycle RVGRM with adiabatic compression and expansion processes.

It should be accepted that this cycle uses the same heat sources with the same temperatures T_C and T_E. The RVGRM cycle implementation with the same temperatures leads to external irreversibility due to the heat transfer in the processes *2'–2* and *4'–4* at finite and fairly large temperature differences.

The cycle is implemented in the range of average planimetric temperatures:

$$\overline{T}_C = \frac{T_C' - T_C}{\ln\left(T_C' / T_C \right)}; \ \overline{T}_E = \frac{T_E - T_E'}{\ln\left(T_E / T_E' \right)} \qquad (12)$$

Using adiabatic processes, it's possible to decrease cycle efficiency significantly.

The states at the beginning and end of the expansion process correspond to the minimum angle between the axes of the vanes in the cavity in question, and therefore to its minimum volume; the cavity increases in the volume (approximately two times or more).

How does pressure vary with volume change during adiabatic expansion can be described as:

$$p_{34'}(\alpha) = p_3\left(\frac{2b-\varphi_v}{2a\cos 2\alpha + 2b - \varphi_v}\right)^k \qquad (13)$$

During expansion process the temperature varies according to the law:

$$T_{34'}(\alpha) = T_3\left(\frac{2b-\varphi_v}{2a\cos 2\alpha + 2b - \varphi_v}\right)^{k-1} \qquad (14)$$

At the moment of the windows opening for the working block connecting with the refrigerator, the process of transferring working fluid begins from one working block to another through the refrigerator with heat supply. In the process of heat supply, pressure and temperature increase. The latter takes the value $\overline{T_E}$.

Let us work out the relationship between the pressure and volume of the utility during adiabatic compression as well:

$$p_{12'}(\alpha) = p_1\left(\frac{2a+2b-\varphi_v}{2a\cos 2\alpha + 2b - \varphi_v}\right)^k, \qquad (15)$$

$$T_{12'}(\alpha) = T_1\left(\frac{2a+2b-\varphi_v}{2a\cos 2\alpha + 2b - \varphi_v}\right)^{k-1} \qquad (16)$$

The design of the cooler provides heat rejection to the environment, where the gas temperature is reduced to a temperature $\overline{T_C}$.

The work done during compression and expansion processes of the working fluid can be represented by certain integrals:

$$A_{com} = \int_0^{\pi/4} p_{12'}(\alpha)\frac{dV(\alpha)}{d\alpha}d\alpha\,, \qquad (17)$$

$$A_{exp} = \int_{3\pi/4}^{\pi} p_{34'}(\alpha)\frac{dV(\alpha)}{d\alpha}d\alpha \qquad (18)$$

For work done in the thermodynamic cycle we have finaly:

$$A_i = A_{com} - A_{exp} \qquad (19)$$

Power at the specified frequency of shaft rotation n will be:

$$W = 4A_i\frac{n}{60}, \qquad (20)$$

where 4 − the number of paired cavities in the two blocks of the refrigerating machine that implement the thermodynamic cycle per shaft rotation.

Integrals (17) and (18) cannot be calculated analytically. Numerical modeling was used to determine them.

4. THEORETICAL RESEARCH OF EFFICIENCY INDICATORS FOR RVGRM

Here are some of the results obtained using the formula (13)-(16). The expansion process in RVGRM proceeds at an angle of rotation of the output shaft 135° ≤ α ≤ 180°.

Fig. 7 shows, during the expansion process in the cavity, the pressure and temperature vary from $p_3(135°) = 12$ to $p_{4'}(180°) = 2{,}85$ bar, and from $T_3(135°) = 173$ to $T_{4'}(180°) = 99{,}4$ K

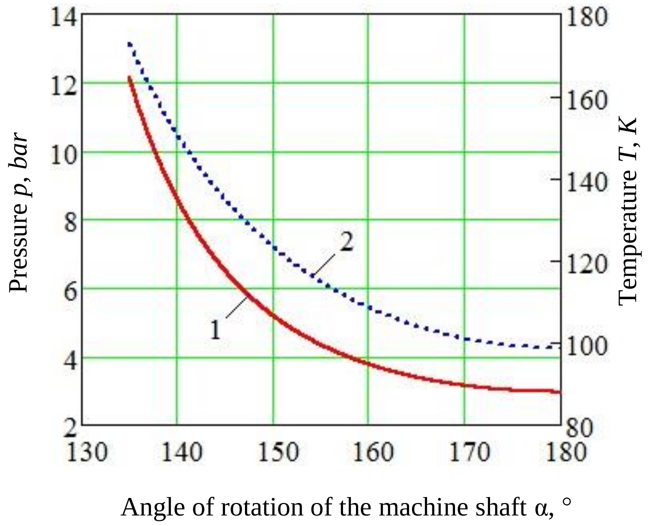

Fig. 7. The change in pressure (1) and temperature (2) in the process of expansion depending on the angle α.

The compression process proceeds in RVGRM at $0° \leq \alpha \leq 45°$ an angle of rotation of the drive shaft. The pressure and temperature are p_1 = 5 bar and T_1 = 300 K at the start of the compression process. The pressure and temperature vary graph in the working cavity is shown in Fig. 8.

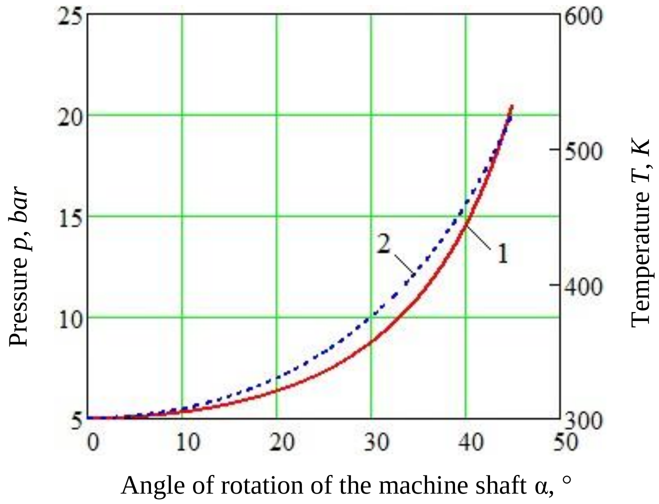

Fig. 8. The change in pressure (1) and temperature (2) in the process of compression depending on the angle α.

It results in pressure and temperature vary in the cavity from $p_1(0°)$ = 5 to $p_{2'}(45°)$ = 20.5 bar, and from $T_1(0°)$ = 300 to $T_{2'}(45°)$ = 525 K.

The performed calculations of the RVGRM cycle characteristics are showed that, taking into account the adiabatic nature of the compression and expansion processes, the degree of thermodynamic perfection decreased to

$$\eta_S = \varepsilon_A / \varepsilon_S = 0,49 / 1,36 = 0,36 \qquad (21)$$

where ε_A − machine cooling ratio with adiabatic processes. The characteristics of the RVGRM cycle are in the provided Table. 1.

Tab. 1 shows the indicators of the RVGRM performance evaluation, obtained as a result of mathematical modeling.

As noted, the developed rotory-vane gas refrigeration machine has several advantages. Refrigeration machine can achieve a high efficiency level in the moderate cold produced.

The research of the RVGRM two-block characteristics in a wide range of its load and speed modes is performed. During analysis it was established the coefficient η_S varies depending on the T_E, that let us to state, the degree of thermodynamic perfection of the RVGRM has an extremum (in this case, a maximum) as a function $\eta_S = f(T_E)$, the Fig. 9 confirms it.

Table 1. Results of mathematical modeling of the RVGRM cycle

Parameter	Value
Average temperature in the volume of the refrigerator $\overline{T_E}$, K	133
Average temperature in the volume of the cooler $\overline{T_C}$, K	402
Maximum pressure p_{max}, bar	20,5
Cooling capacity Q_E, kW	12
Thermal load on the cooler Q_C, kW	36,5
Power consumption W, kW	24,5
Coefficient of performance ε_A	0,49
Degree of thermodynamic perfection η_S	0,36

Fig. 9 shows that the optimum value of the cooling temperature T_{Eopt}≈ 233 K, at present value of η_S was 0,476.

The values obtained η_S big enough and it should be taken into account, that all calculations were carried out with the application of the adiabaticity for the compression processes of and expansion of the working fluid and high-performance rotary-vane design made of low-alloy steel.

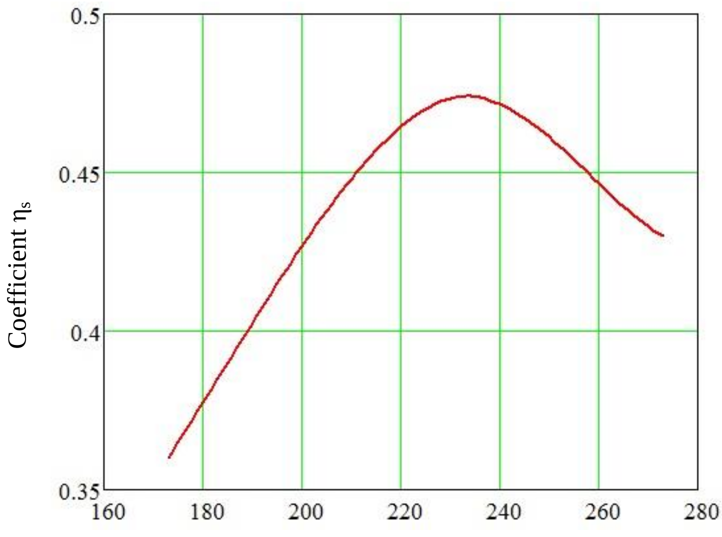

Fig. 9. The dependence of the coefficient η_S at cooling temperature T_E.

In the first copies of Stirling machines T_{Eopt}≈ 130 K, wherein the values η_S equal 0,22 [20]. In [21] the optimal temperature range is indicated, which is produced by Stirling refrigeration machine (cold from 233 to 73 K).

A comparison of the Stirling refrigeration machine parameters with RVGRM was carried out. Tab. 2 shows the results of a parameters comparison for the serially produced Stirling refrigeration machine with RVGRM.

Table 2. The results of the parameters comparison for the SRM with RVGRM

Parameter	SPC-1	SRM-9000/80	RVGRM
Cooling capacity Q_E, kW	12	12	12
Shaft rotation frequency n, min^{-1}	1450	1450	1200
Degree of thermodynamic perfection η_S	0.31	0.3	0.36
Cooling temperature T_E, K	173	173	173
Working fluid	Helium	Helium	Helium
Maximum pressure p_{max}, MPa	5	5	2
Number of cylinders	4	4	2
Expansion cavity volume V_e, см^3	1000	980	1003
Weight, kg	250	1500	100

At the same cooling capacity Q_E = 12 kW the efficiency of the RVGRM is higher by 15% in comparison with the piston serially produced Stirling refrigeration machine. By mass characteristics RVGRM compared with SPC-1 "Stirling Cryogenics» 2.5 times less than, and compared to SRM-9000/80 «Geliymash» 15 times less than. The search for compactness in RVGRM is the goal achieved: 510mm × 560mm × 300mm (L×W×H).

The RVGRM performance analysis has been done with the use of various working fluids (helium, nitrogen, methane) at a temperature level of 233 K. It is proved that for each from working fluids the cooling capacity increases with the shaft rotation frequency vary and the charging pressure increase (see Fig.10, Fig.11).

For helium use, the cooling capacity of Q_E = 13215 W, and the cooling coefficient ε = 1.656. When using nitrogen, the cooling capacity is decreased to 9156 W, which is 30% less compared with the helium use, and the maximum value of ε = 1.54, which is 6% less than for helium.

In the case of methane using, the cooling capacity decreased to 12050 W, which is 9% less compared to the helium use. The maximum value of ε = 1.45, which is 12% less than for helium.

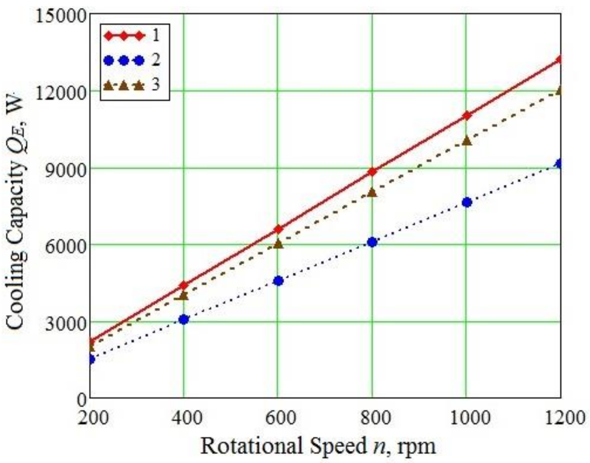

1 – helium, 2 – nitrogen, 3 – methane.

Fig.10. Comparison refrigerating performance Q_E from the frequency of rotation n for working fluids.

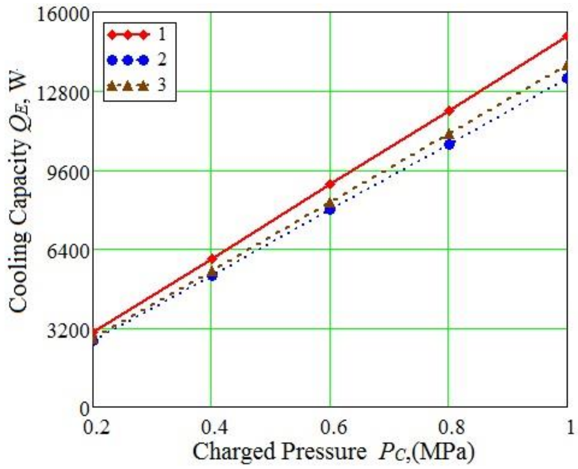

1 – helium, 2 – nitrogen, 3 – methane.

Fig.11. Comparison refrigerating performance Q_E from the charging pressure P_c for working fluids.

For helium use, the cooling capacity of Q_E = 13215 W, and the cooling coefficient ε = 1.656. When using nitrogen, the cooling capacity is decreased to 9156 W, which is 30% less compared with the helium use, and the maximum value of ε = 1.54, which is 6% less than for helium.

In the case of methane using, the cooling capacity decreased to 12050 W, which is 9% less compared to the helium use. The maximum value of ε = 1.45, which is 12% less than for helium.

The difference in machine performance between nitrogen and helium use is due to the pressure drop in the system from the compression cavity into the expansion cavity and the general significant drop in nitrogen pressure compared to helium.

5. RVGRM DESIGN

RVGRM at low cooling temperatures can be an alternative to cascade vapor compression refrigerating machines. Cause of its use for low temperatures is advisable for two reasons: partly high thermodynamic efficiency; there is no need to use two-stage compressors, which significantly increase the VCRM cost.

In RVGRM, the cam mechanism for converting motion is used to increase the smoothness of movement of the vanes. In the mechanism there are no complex gears. The design of the RVGRM allows to ensure relatively good efficiency due to the its compactness in working chambers and reduction of the length of the pipelines. The machine has the ability to regulate the cooling capacity by varying the gas pressure and temperature in the working volume of the refrigerating machine. It is achieved by the structural optimization, adding system elements as a receiver, compressor and a controlled valve. Fig. 12 shows the machine elements of the rotary-vane diblock GRM.

RVGRM consists of two working units – blocks. Each block contains cylinders 1 and 2, two side covers 3 and 4, coaxial shafts 5 and 6, rotors 7 and 8, made integral with the specified shafts. The vanes 9 and 10 are mounted on the rotors 7 and 8 and placed in the cylinder 1. The cylinders 1 and 2, the side covers 3 and 4, the rotors 7, 8 and the vanes 9 and 10 form four working cavities 11, 12, 13, 14 (15, 16, 17, 18) in each cylinder (see fig. 2). The cylinders are provided windows 19-22, which are connected through-passages cold working fluid 23-26 with a refrigerator 27, as well as the through-passages of the compressed working fluid 28-31 - with a cooler 32. The windows 21 and 22 of cylinder 1 are connected by lines 23-26 with the same windows 21 and 22 in cylinder 2 to create a counter-current through refrigerator 27 (see Fig. 12 and 13).

Windows 19 and 20 of cylinder 1 are intersected by through-passages 28-31 with the same windows 19 and 20 of cylinder 2 with the formation of counterflow through cooler 32.

The working cavities of the cylinders 1 and 2, the lines of the cooler 32 and the refrigerator 27 are sealed and filled under excess pressure with a gaseous working fluid, such as helium.

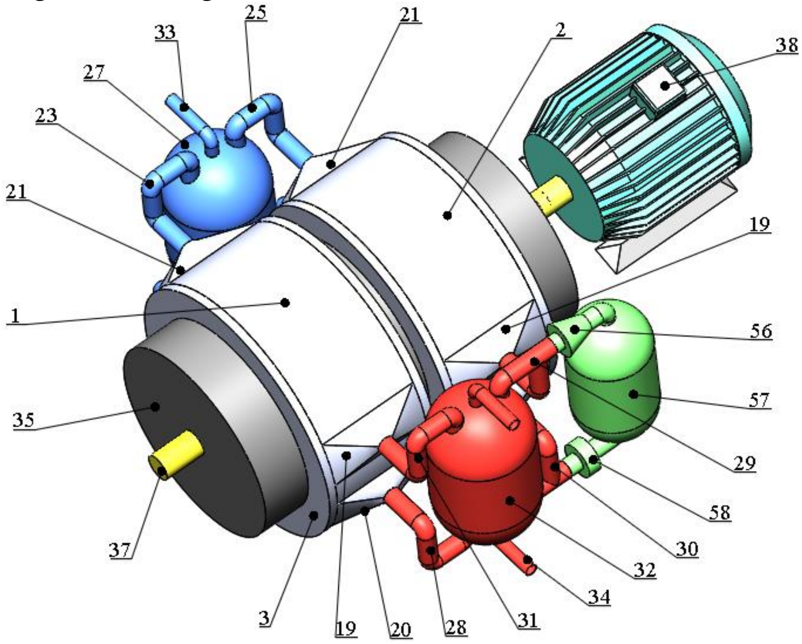

Fig. 12. The design of the two-block RVGRM.

Heat is supplied from the cooled object to the working fluid through line 33, which is connected to the refrigerator 27, and heat is rejected from the working medium through line 34, which is connected to the cooler 32. On both sides of the working blocks 1 and 2 are installed mechanisms for he conversion motion of 35 and 36, which are rigidly connected to each other by one common drive shaft 37 associated with the electric motor 38.

MCM 35 converts a uniform rotational motion of the drive shaft 37 into a rotational - oscillatory motion of the rotors 7 and 8 with the vanes 9 and 10. This ensures smooth and unstressed operation of the refrigeration machine.

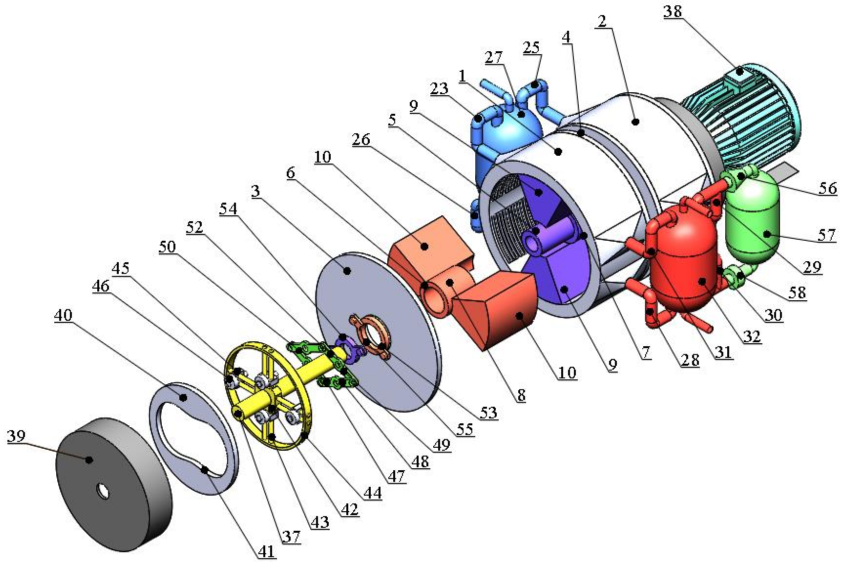

Fig. 13. General view of RVGRM with spaced construction details.

The MCM contains a corpus 39, a disk 40 is rigidly fixed on the wall of it. In the center of the disk a shaped contour 41 is made (see Fig. 13).

MCM 35 converts a uniform rotational motion of the drive shaft 37 into a rotational - oscillatory motion of the rotors 7 and 8 with the vanes 9 and 10. This ensures smooth and unstressed operation of the refrigeration machine. The MCM contains a corpus 39, a disk 40 is rigidly fixed on the wall of it. In the center of the disk a shaped contour 41 is made.

On the drive shaft 37 of the refrigerating machine, the hub 42 is rigidly fixed with four pairs of guides 43 and a flywheel 44. Between the guides 43 are sliders 45 with fingers that move along the guides 43. Approaching the center of the hub 42, they slow down their movement, and moving away from the center of the hub 42 - accelerate it. At one end of the fingers of the sliders 45 are fixed rollers 46, which are in contact with the profiled loop 41. On the opposite side of the fingers of the sliders 45 are the hinges of the peaks of the main slave link 47, which consists of four links of the same length 48-51. The link 47 centers links pivotally connected with the levers 52 and 53 of the coaxial shafts 54 and 55. These shafts are rigidly connected with the coaxial shafts 5 and 6 of the working block 1.

To regulate the cooling capacity of the machine, a working compressor 56 is connected to the line 29, which is connected to the receiving receiver 57, which is connected to the line 30 by a controllable valve 58 (Fig. 13).

6. CONCLUSIONS

The research done allows to develop theoretical bases for calculation, design and construction of rotary vane gas refrigerating machine intended for the cold production at temperature level from 0°C to -100°C. A set of scientific and applied problems that are relevant for refrigeration technology has been solved, allowing further improvement of the design characteristics for these machines, reasonably choosing and implementing the optimal modes of their operation.

The design techniques development and additional research it is a necessary complex and the basis for the improvement of the new rotary vane gas refrigerating machine. The main results obtained during the execution of this study can be formulated as follows:

1. Stirling refrigerating machine, created by a number of companies for the production of moderate cold, have satisfactory characteristics. However, their further improvement is constrained by the disadvantages caused by the use of a crank mechanism in these machines. The orientation on the SRM rotory-vane design eliminates the drawbacks of traditional Stirling machines. In addition, the rotary-vane machine has significant reserves for their further improvement in order to create a generation of new efficient and reliable refrigeration machines.

2. The mechanism used in the studied refrigeration machine to convert the rhomboid rotation into the rotational-oscillatory movement of rotors with vanes ensures the harmonious nature of smooth movement without vibrations, changes in the volume of cavities in two working blocks connected to each other. The optimum shift of the experimental values of volumes in blocks, which are functions of the rotation angle of the drive shaft is equal to $\pi/4$.

3. Work processes in RVGRM are described by a system of differential equations that do not allow their analytical solution. To determine the energy characteristics of the refrigerating machine, a mathematical model was developed and implemented for describing working processes that take into account the variability of gas mass in paired cavities and changes depending on the angle of rotation of the drive shaft, pressures and temperatures of the working fluid.

4. To ensure the design and technological unification of parts and assemblies of rotary-vane refrigerating machines of various cooling capacities by their solid-state models are created. This allows the development of RVGRM the number of connected parts and assemblies left unchanged. The ratio of the equivalent working volume to the volume of the machine (the coefficient of compactness of the main volume) of the RVGRM, as compared to traditional Stirling refrigerating machines, will be at the level of 15-20%.

5. Analysis of the losses from thermodynamic irreversibility in the RVGRM shows that it is necessary to reduce them to ensure the highest possible intensity of heat exchange between the working fluid of the machine and the upper and lower heat sources. For this purpose, a cooler and refrigerator must be made in form multiflow plate-fin heat exchangers (three streams).

6. The energy characteristics of rotary-vane gas refrigerating machines were determined using three working fluids: helium, nitrogen, methane. Comparison of machines for the main characteristics showed that helium is no alternative. So, when converting a machine from helium to nitrogen, its cooling capacity decreases by 30%, and the maximum value of the coefficient of perfomance decreases by 6%; when methane is used, the cooling capacity is 9% less than in helium RVGRM.

7. In Stirling refrigerating machine heat recovery is organized in the isochoric process. This process is implemented in the regenerator of the machine, which has a heat and heat intensive nozzle. In the design of RVGRM, the quasi-isochoric process of heat recovery is carried out using the heat-intensive mass of the two vanes of the machine. This allows you to create a continuous movement of the flow of the working fluid towards each other in the cooler and refrigerator.

8. In order to assess the life cycle RVGRM analyzed the impact on the environment the main stages of the life of the product, including the purchase of raw materials, production, system operation, maintenance, etc. Based on the analysis, it was determined that the production, installation, operation and disposal RVGRM causes 37% less harmful effect on the environment compared with the Stirling refrigerating machine SPC-1.

REFERENCES

[1] A.T.A.M. de Waele. Basic operation of cryocoolers and related thermal machines. *Journal of Low Temperature Physics*, 2011, vol. 164, no. 5-6, pp.179-236. doi.org/10.1007/s10909-011-0373-x.

[2] Thombare D.G., Verma S.K. Technological development in the Stirling cycle engines. *Renewable and Sustainable Energy Reviews*, 2006, vol. 12, no. 1, pp. 1-38.

[3] Sun Le'an, Zhao Yuanyang, Li Liansheng, Shu Pengcheng. Performance of a prototype Stirling domestic refrigerator. *Applied Thermal Engineering*, 2008. vol. 29, pp. 210-215.

[4] Osorio M.R., Morales A.P., Rodrigo J.G., Suderow H., Vieira S. Demonstration experiments for solid-state physics using a table-top mechanical Stirling refrigerator. *European Journal of Physics*, 2012, vol. 33, no. 4, pp.757-770. doi.org/10.1088/0143-0807/33/4/757.

[5] Sun J.F., Kitamura Y., Satake T. Application of Stirling cooler to food processing: Feasibility study on butter churning, *Journal of Food Engineering*, 2008, vol. 84, no. 1, pp. 21-27.

[6] Chakravarthy V., Shah R., Venkatarathnam G. A review of refrigeration methods in the temperature range 4-300 K. *Journal of Thermal Science and Engineering Applications*, 2011, vol. 3, no. 2. doi:10.1115/1.4003701.

[7] Xiaoqin Yang, Chung J. N. Size effects on miniature Stirling cycle cryocooler. *Cryogenics*, 2005, vol. 45, pp. 537-545.

[8] Welty S. C., Cueva F. Energy efficient freezer installation using natural gas and a free piston Stirling cooler [VI International Refrigeration and Air Conditioning Conference]. Trabajo, 2001. No. 96, pp. 199-208.

[9] Yong- Rak Kwon, Berchowitz D.M. Operational characteristic of Stirling Machinery [International Congress of Refrigeration]. Washington, D.C., 2003.

[10] Lavrenchenko G.K. Refrizheratoryi Stirlinga i drugie KGM: Razvitie ih teorii nauchnoy shkoloy professora V.S. Martyinovskogo [Stirling refrigerators and other cryogenic gas machines. Development of their theory by the scientific school of Professor V.S. Martynovsky]. *Kholodilnaya tekhnika – Refrigeration Engineering*, 2017, no.1, pp. 50-56. (In Russian).

[11] Lavrenchenko G.K. Refrizheratoryi Stirlinga i drugie KGM: Razvitie ih teorii nauchnoy shkoloy professora V.S. Martyinovskogo [Stirling refrigerators and other cryogenic gas machines. Development of their theory by the scientific school of Professor V.S. Martynovsky]. *Kholodilnaya tekhnika – Refrigeration Engineering*, 2017, no.2, pp. 48-53. (In Russian).

doi.org/10.1016/j.applthermaleng.2008.02.036.

[12] Kaushik S.C., Tyagi S.K., Bose S.K., Singhal M.K. Performance evaluation of rereversible Ericsson and Stirling heat pump cycles, *International Journal of Thermal Sciences*, 2002, vol. 41, pp. 193-200.

[13] Wunderlich W. Single-disk cam mechanism with oscillating double roller follower. *Mechanism and Machine Theory*, 1984, vol. 19. no. 4/5, pp. 409-415.

[14] Kongtragool B., Wongwises S. Thermodynamic analysis of a Stirling engine including dead volume of hot space, cold space, and regenerator. *Renewable Energy*, 2006, vol. 31, pp. 345-359.

[15] Tyagi S.K., Kaushik S.C., Singhal M.K. Parametric study of irreversible Stirling and Ericsson cryogenic refrigeration cycles, *Energy Conversion and Management*. 2002, vol. 43 no. 17, pp. 2297–2309.

[16] Huang B.J., Chen H.Y. Modeling of integral-type Stirling refrigerator using system dynamics approach. *International Journal of Refrigeration*. 2002, vol. 23, no. 8, pp. 632-641.

[17] Cha J. S., Ghiaasiaan S.M., Kirkconnell C.S. Longitudinal hydraulic resistance parameters of cryocooler and Stirling regenerators in periodic flow. *Advances in Cryogenic Engineering*, 2008, vol. 53, pp. 259-266.

[18] Ö. Ercan Ataer, Karabulut H. Thermodynamic analysis of the V-type Stirling cycle refrigerator. *International Journal of Refrigeration*. 2005, vol. 28. no. 2, pp. 183-189.

[19] Tekin Y., Ataer O.E. Performance of V-type Stirling-cycle refrigerator for different working fluids. *International Journal of Refrigeration*, 2010, vol. 33, no 1, pp. 12-18.

[20] McFarlane P., Semperlotti F., Sen M. Mathematical model of an air-filled alpha Stirling refrigerator. *Journal of Applied Physics*, 2013, vol. 114. doi.org/10.1063/1.4824536.

[21] Ki T., Jeong S. Step-by-step design methodology for efficient Stirling-type pulse tube refrigerator. *International Journal of Refrigeration*. 2012. vol. 35, no. 4, pp. 1166-1175. doi.org/10.1016/j.ijrefrig.2012.01.017.

[22] ISO. ISO 14040-environmental management – life cycle assessment – principles and framework. Geneva, 2006.

[23] ISO. ISO 14044-environmental management – life cycle assessment – principles and framework. Geneva, 2006.

[24] Greening B., Azapagic A. Domestic heat pumps: Life cycle environmental impacts and potential implications for the UK. *Elsevier*. 2012, vol. 39, pp. 205-217. doi:10.1016/j.energy.2012.01.028.